Supplementary Material: Reservoir computing using spin-VCSELs - the influence of timescales and data injection schemes

Lukas Mühlnickel, Jonnel A. Jaurigue, Lina C. Jaurigue,* and Kathy Lüdge†

Technische Universität Ilmenau, Institut für Physik, Weimarer Straße 25, 98693 Ilmenau, Germany

(Dated: April 29, 2024)

I. SUPPLEMENTARY

A. Dynamics and Performance with higher Birefringence

In the main paper the reservoir computing dynamics and performance have been investigated in the injection parmeter space. The shift of the locking cone with higher birefringence was discussed and Fig.1 now presents the full scans that were the basis for parts of the the histograms presented in the main paper. In detail, Fig.1 shows the color coded emission dynamics of the spin-VCSEL (a), the performance with carrier (b) and phase (c) injection for a birefringence value of $\gamma_p = 30\,ns^{-1}$. The locking is shifted to lower frequency detunings due to the change in the laser frequency. Besides that an improvement in the overall performance can be seen for both injection schemes if compared to $\gamma_p = 1\,ns^{-1}$. For carrier injection the optimal regions shift to higher injection strength. The inset show zooms ino the best performing regions.

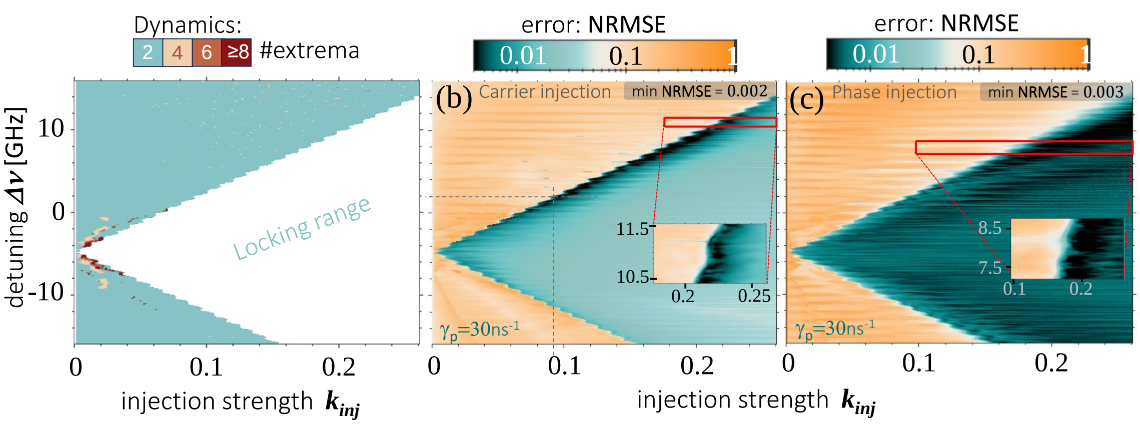

Figure 1. a) Spin VCSEL dynamics found in the injection parameter space of injection strength k_{inj} and detuning $\Delta\nu$ ($k = 0.0022, \gamma_p = 30\,ns^{-1}$ (same rotating frame as for $\gamma_p = 1\,ns^{-1}$, and not corrected for the shift in laser frequency γ_p). b,c) NRMSE error with carrier and phase injection, respectively. Insets show zooms into good performing regions. Minimum error is given on the top right inset.

B. Impact of Virtual Node Distance on Performance

In the main text we state that an optimal virtual node distance is given by a value of $\theta = 33\,ps$. Figure 2 shows the performance as a function of the clock cycle T and the delay time τ. virtual node distance θ (the median value after averaging over 10 different masks is plotted). The number of virtual nodes N_v is not changed in order to not mix the results with the effect of an increasing readout dimension [1, 2]. This means that changing T effectively changes the virtual node distance θ. In the figure it can be seen that the ratio between clock cycle and delay time dramatically change the performance as was also discussed elsewhere [1, 3]. The dark regions of good performance are centered around a ratio of $\tau/T \approx \sqrt{2}$ which has been proven before to be a good choice [1, 3]. For the phase injection that is

* Email address: lina.jaurigue@tu-ilmenau.de

† Email address: kathy.luedge@tu-ilmenau.de

plotted in Fig.2a, a faster readout is possible (see red star) while for carrier injection longer clock cycle values and thus longer θ are better. Comparing the minimum performance values possible the phase injection is much better at this very high injection strength of $k_{inj} = 0.22$ for smaller injection strength of $k_{inj} = 0.059$ as also discusse din the main paper, the carrier injection leads to the overall best results (Fig.3).

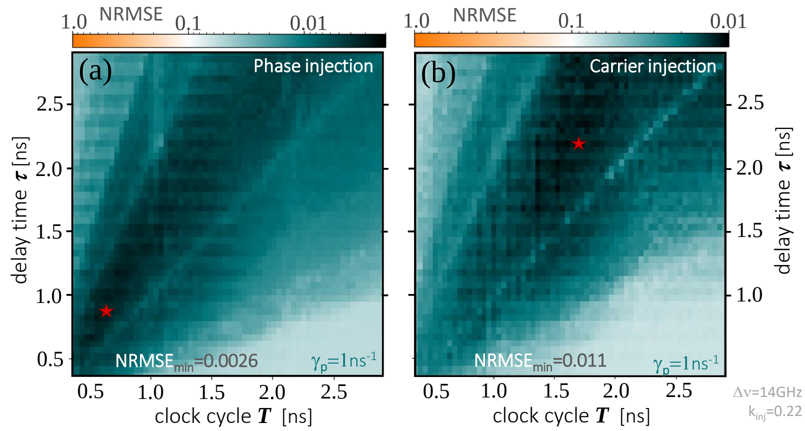

Figure 2. Prediction performance NRMSE error as a function of the delay time τ and the clock cycle $T = 30 \times \theta$. (a) phase injection scheme (b) carrier injection scheme for $\gamma_P = 1\,ns^{-1}, \Delta\nu = 14GHz, k_{inj} = 0.22$

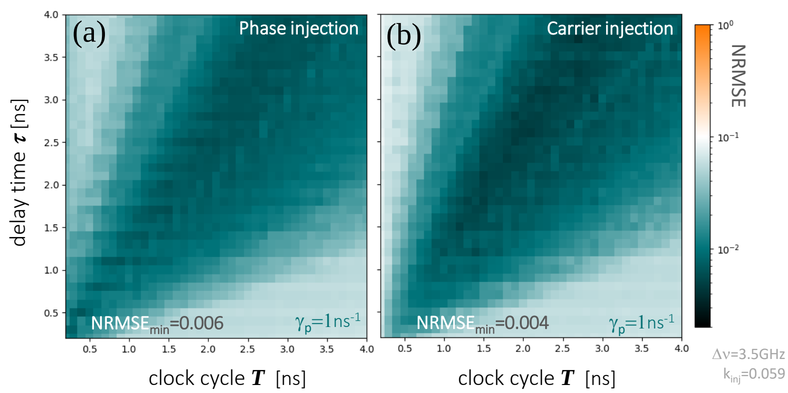

Figure 3. Prediction performance NRMSE error as a function of the delay time τ and the clock cycle $T = 30 \times \theta$. (a) phase injection scheme (b) carrier injection scheme for $\gamma_P = 1\,ns^{-1}, \Delta\nu = 3.5GHz, k_{inj} = 0.059$

C. Different tasks, spin relaxation time and modulation response

Throughout the paper we used a one step ahead prediction task for the x-coordinate, i.e. the output of the laser intensity is used to predict one discrete time step $\Delta_d = 0.1$ of the Lorenz x-coordinate into the future. In Fig.4b we show its prediction performance as a function of the spin relaxation time for carrier injection into m (orange curve) but we also show the more complicated cross-prediction task were the z-coordinate is to be predicted after injecting the x-coordinate (green line). Here a smaller time step of $\Delta_d = 0.02$ is used. Overall a similar dependence on the spin relaxation rate is found. For the phase injection scheme, instead, the spin relaxation does not change the performance as can be seen by the green line in Fig.4a.

In Fig.4c we depict the modulation response of the solitary spin-VCSEL color coded as a function of the spin relaxation rate γ_s. We can see that the additional resonance at a modulation frequency of 8 GHz decreases with γ_s and for values $\gamma_s > 400\,ns^{-1}$ only the peak resulting from the relaxation oscillation at $3GHz$ remains.The fast beating oscillation are exploited for the case of carrier injection but they are not addressed for phase injection.

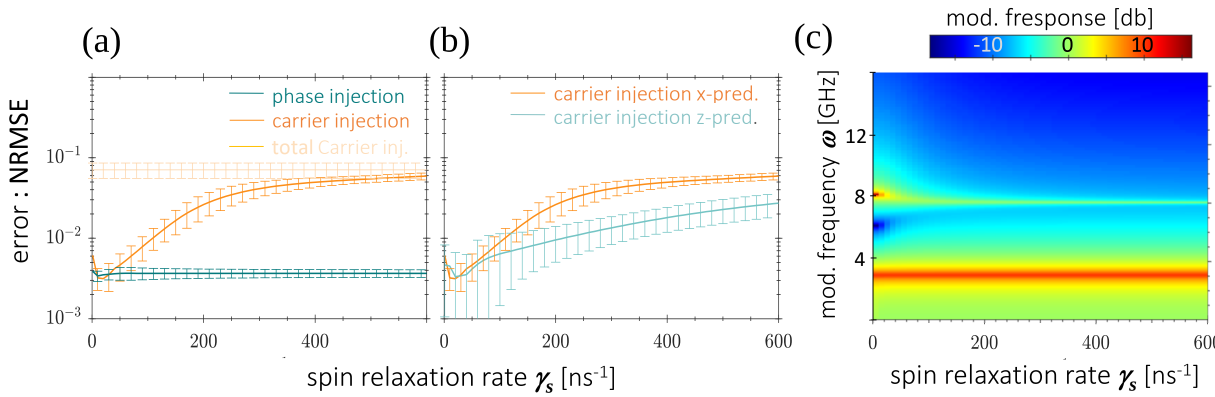

Figure 4. Impact of spin relaxation rate: Computing error as a function of γ_s for a) carrier-, phase and total carrier injection (orange, green and light orange curve), b) two different prediction task (orange: x-prediction (stepsize 0.1) and green: z-prediction (stepsize 0.02), c) modulation response of the solitary spin-VCSEL after modulating the pump polarization (color code indicates the normalized modulation response in db). Parameters: $\gamma_p = 30\,ns^{-1}$, $k = 0.0022$; .

II. REFERENCES

[1] A. Röhm, L. Jaurigue, and K. Lüdge, Reservoir computing using laser networks, IEEE J. Sel. Top. Quantum Electron. **26**, 7700108 (2019).

[2] F. Köster, S. Yanchuk, and K. Lüdge, Insight into delay based reservoir computing via eigenvalue analysis, J. Phys. Photonics **3**, 024011 (2021).

[3] T. Hülser, F. Köster, L. Jaurigue, and K. Lüdge, Role of delay-times in delay-based photonic reservoir computing, Opt. Mater. Express **12**, 1214 (2022).